

## Design and Performance of Inductive Electrostatic Sprayer

<sup>1</sup>Weidong Jia, <sup>1</sup>Fei Xue, <sup>1</sup>Baijing Qiu and <sup>2</sup>Zhentao Wang

<sup>1</sup>Key Laboratory of Modern Agricultural Equipment and Technology, Ministry of Education, Jiangsu University, Zhenjiang 212013, China

<sup>2</sup>College of Energy and Power Engineering, Jiangsu University, Zhenjiang 212013, China

**Abstract:** In order to improve spraying results, an inductive electrostatic sprayer was designed. The performance of the sprayer was then tested. The test result shows that the charge-to-mass ratio can reach 0.951 mc/Kg when electrostatic voltage is 20 KV and working pressure is 0.25 to 0.4 MPa. The particle size distribution of charged droplets are more concentrated than that of uncharged droplets, the axial velocity of charged droplets is faster than that of uncharged droplets, and the velocity distribution uniformity is also improved. The average deposition rate under charging conditions is 14% higher than that in uncharged conditions. Moreover, the deposit rate of the back of the leaf is evident.

**Keywords:** Axial velocity, charged droplets, charge-to-mass ratio, deposition rate, electrostatic spray, particle size

### INTRODUCTION

Electrostatic spray technology has superior performance in improving droplet size, size distribution and deposit rate on targets, adsorption, and uniformity. Therefore, this technology has long been used in plant protection and epidemic prevention (Wang *et al.*, 2008; Wang *et al.*, 2004; Edward, 2001). The use of electrostatic spray in various fields has been developed in numerous countries. An example is Electrostatic Spraying System, Inc., which has developed a small electrostatic sprayer (Shu *et al.*, 2002). On the other hand, electrostatic sprayers and other large sprayers in China are mostly used in the prevention and control of forestry. The small electrostatic sprayers are not widely used (Kang *et al.*, 2007).

Electrostatic sprayers come in different types and structures. However, the electrostatic nozzle and electrostatic generator, which are indispensable components, remain the same for all sprayer types. The measurement parameters of used for electrostatic sprayers are charge-to-mass ratio, particle size, velocity of droplets, and deposit rate of pesticide.

An inductive electrostatic sprayer was developed based on the above background as well as on earlier theories. The performance of the electrostatic sprayer was finally analyzed by testing its charge-to-mass ratio, particle size, velocity of droplets, and deposit rate of pesticide.

### WORKING PRINCIPLE AND STRUCTURE OF MACHINES

**Working principle:** The three kinds of charging methods for an electrostatic sprayer are corona, contact,

and induction charging. Induction charging has low charging voltage, and this method is the safest of the three. Insulation is easy to implement because the electrodes of the sprayer and the droplets are separated (Edward, 2001; Lv, 2009). Figure 1 shows the working principle of the inductive electrostatic sprayer. The anode grounding and the negative electrode of the electrostatic generator combine with annular electrodes. The pesticide pumped from the tank through a nozzle forms droplets. The electric field between the electrode and the liquid jet charges the droplet induction. The negative charge of the droplets can be attributed to the attraction to positively charged objects, which facilitates directional movement adsorption on the surface of the target.

**Machine structure:** Figure 2 shows the configuration of the inductive electrostatic sprayer. The sprayer primarily comprises a frame, battery, high-voltage electrostatic generator, pressure-regulating valve, diaphragm pump, liquid tank, spray gun, and electrostatic nozzle. Figure 3 shows the three-dimensional structure of the electrostatic nozzle. The liquid tank is located in front of the barrow. The diaphragm pump is located in a seal box to prevent contact with the liquid, battery, high-voltage electrostatic generator, and pressure-regulating valve. One side of the seal box has a small door, which is convenient for battery charging and pressure adjustment. The electrostatic nozzle is on one end of the spray gun, whereas the opposite end contains a fluid pipe and wire. The fluid pipe is connected to the diaphragm pump, whereas the wire is connected to the high-voltage electrostatic generator. The fluid pipe and wire, both of which are exposed outside the box, are

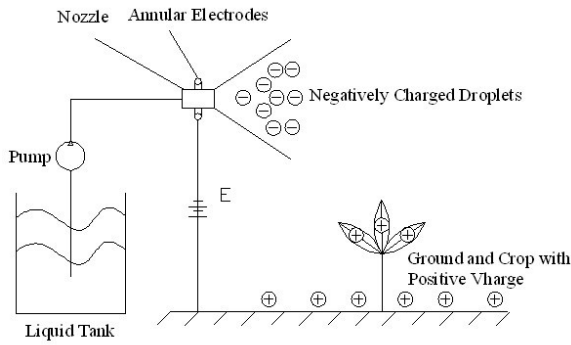


Fig. 1: Working principle of the inductive electrostatic sprayer

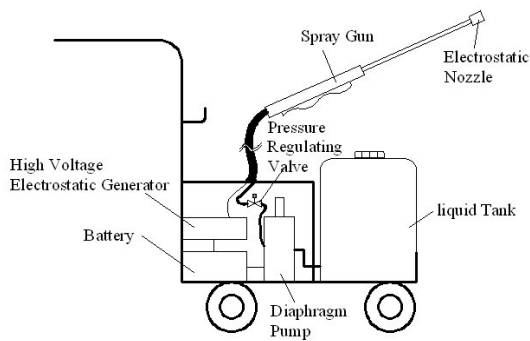


Fig. 2: Configuration of the inductive electrostatic sprayer

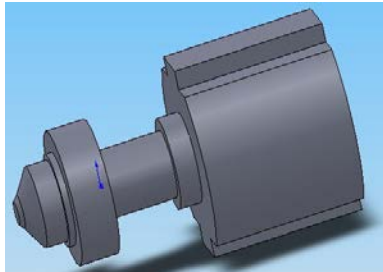


Fig. 3: Electrostatic nozzle

Table 1: Main parameters of the inductive electrostatic sprayer

Item	Parameter
Liquid tank's capacity/L	50
Flow/L*/h	5-7
Nozzle pressure /MPa	0.25-0.4
Static voltage /KV	20

covered by an insulating material. The left wall of the frame has a pair of hooks, on which the spray gun can be hung after use. Table 1 shows the main parameters of the inductive electrostatic sprayer.

### EXPERIMENTAL DEVICE AND MEASUREMENT METHOD

**Charge-to-mass ratio:** Charge-mass ratio refers to the ratio of charge quantity  $Q$  to droplet quality  $m$ , which is an important parameter for the measurement of the

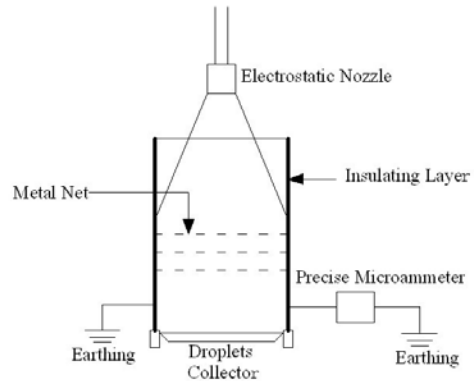


Fig. 4: Device used to measure charge-to-mass ratio

droplet charged effect. The formula for charge-to-mass ratio  $A_Q$  is (Jia *et al.*, 2007; Jia *et al.*, 2008; Wen *et al.*, 2003; Yuan *et al.*, 2000):

$$A_Q = \frac{Q}{m} = \frac{It}{m}$$

where,

$I$  = Denotes the discharge current value of charged droplets,

$M$  = The quality of the group of droplets

$t$  = The measuring time

The three methods for measuring charge-to-mass ratio are the mesh target, Faraday cylinder, and simulate the target methods. The proposed device uses the Faraday cylinder method to measure charge-to-mass ratio under different pressures. Figure 4 shows the measuring device.

**Droplet size and droplet speed:** The differences between charged and uncharged droplets in terms of spray width, size, and velocity distribution were compared by using PDPA(Phase Doppler Particle Analyzer) to test the spray flow field (Dantec Company, speed range: 0 m/s to 500 m/s; particle size measurement range: 0.5  $\mu\text{m}$  to 13000  $\mu\text{m}$ ; measurement accuracy: 0.5%; maximum concentration: 106/cm<sup>3</sup>)

**Test and measurement conditions:** Table 2 shows the test and measurement conditions.

**Measuring point arrangement:** The device adopts two-dimensional measurement. The emission light path systems are  $U_y$  and  $U_z$ , which correspond to wavelengths that are 488 and 541.5 nm. The receiving angle is 150°. The focal length of the emission lens is 1000 mm; whereas that of the receiving lens is 500 mm. Sampling time was set at 30s. Figure 5 shows the PDPA test device of the spray flow field. The center line along the spray field is longitudinal in direction and is transverse along the emission probe. The vertical and horizontal intersection and the node in the horizontal

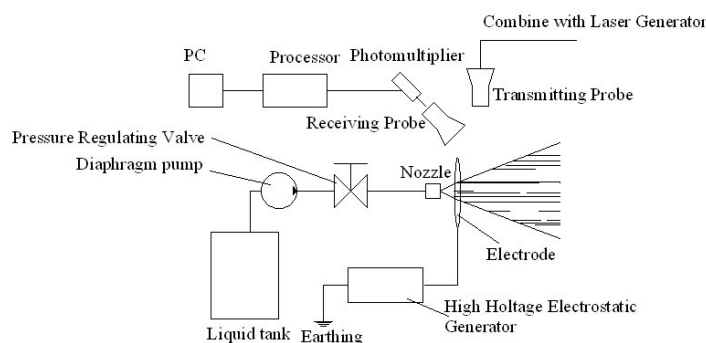


Fig. 5: PDPA test device of spray flow field

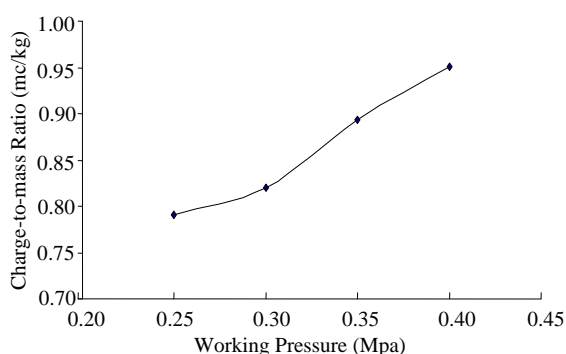


Fig. 6: Charge-to-mass ratio results

Table 2: Test and measurement conditions

Test condition	Measurement condition
Ambient temperature °C	26±1
Relative humidity	70%
Dispersion medium	Air
Dispersing agent	Nothing
Spray medium	21°C Water
Spray refractive index	1.00
Pressure/MPa	0.3

coordinate are zero. A total of 11 measuring points were identified from -100 mm to 100 mm. Particle size was measured at zero point.

**Deposition rate:** The deposition rates of charged and uncharged droplets were tested to prove the charged effect. An experimental plant with a height of 1.5 m was selected as spray object. The plant was divided into three layers. Each layer has a peripheral and an internal component. The upper and the lower layers have four sampling points. Both sides of the leaves are covered with cellophane with a radius of 4.5 cm. The nozzle is placed in a horizontal position and aimed at the center of the plant. A concentration of 500 g/mL of Rh-B solution was used to simulate pesticide. Each test was run for 6 s. Cellophanes are removed and then placed in plastic bags at the end of each spray cycle. The cellophanes were then replaced at each corresponding

position. Elute cellophane solution was used after the experiment to process, analyze, and calculate the Rh-B solution obtained from cellophane by using a spectrophotometer. The deposition rate of plant droplets was then determined by using the following formula:

$$\beta_{dep\%} = \frac{(\rho_{smpt} - \rho_{blk}) \times F_{cal} \times V_{dil} \times 10000}{\rho_{spray} \times A_{col} \times \beta_V}$$

where,

- $\beta_{dep\%}$  = The deposition rate, %
- $\rho_{smpt}$  = The spectrophotometer reading of the test sample
- $\rho_{blk}$  = The blank value of the diluted water elution receiver
- $F_{cal}$  = The correction factor
- $V_{dil}$  = The volume of elution water, L
- $\rho_{spray}$  = The spray concentration, g/L
- $A_{col}$  = The receiver area, cm<sup>2</sup>
- $\beta_V$  = The spray amount, L/ha, 1 ha = 104 m

## RESULTS AND ANALYSIS

**Charge-to-mass ratio** Figure 6 shows the relationship between charge-to-mass ratio and working pressure. The diagram shows that the charge-to-mass ratio linearly increases with working pressure. When working pressure is 0.4 MPa, charge-to-mass ratio reaches the highest value at 0.951 mc/Kg because under high pressure and as liquid flows from the nozzle, a significant difference exists between internal and external pressure. The strong force of percussion with the air facilitates the fracturing of atomized pressure into fine droplets (Jia *et al.*, 2008), thus improving the effect of droplet charged. Therefore, an appropriate increase in working pressure improves charge-to-mass ratio.

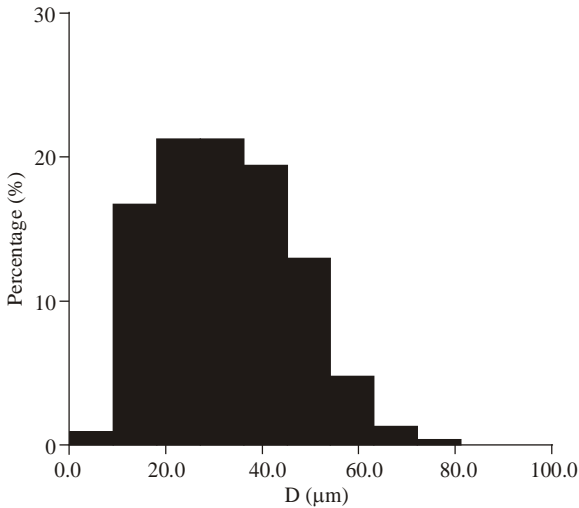


Fig. 7: Particle size distribution of uncharged droplets

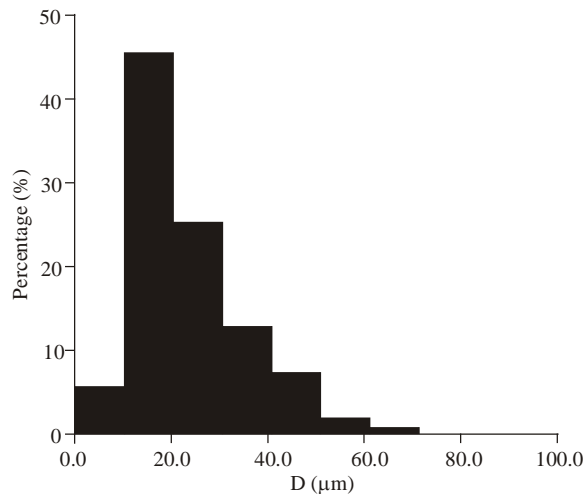


Fig. 8: Particle size distribution of charged droplets

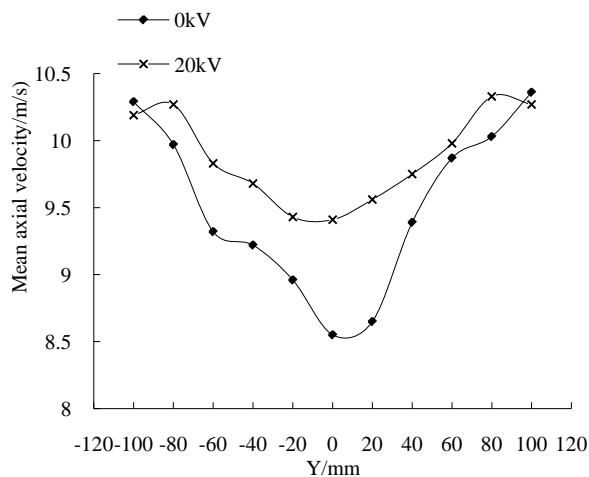


Fig. 9: Distribution of mean axial velocity of charged and uncharged droplets

Table 3: Droplet size of charged and uncharged droplets

Droplets size (μm)	Uncharged droplets	Charged droplets
$D_{10}$	28.1	18.2
$D_{30}$	34.8	26.1
$D_{32}$	42.3	36.7
$D_{43}$	59.2	50.0

**Particle size distribution:** PDPA was used to detect droplet size of charged and uncharged droplets to validate the influence of charged droplets on particle size. Table 2 shows particle sizes of charged and uncharged droplets.  $D_{10}$  refers to the sum of all droplet sizes divided by the total number of droplets, which is called the average diameter.  $D_{30}$  indicates that the volume of the diameter of droplets is equal to the average volume of all droplets, which is called the mean-volume diameter.  $D_{32}$  implies that the surface of the diameter of droplets is equal to the average of all droplet surfaces, which is called the Sauter mean diameter.  $D_{43}$  is the average diameter often used in laser particle-size analysis systems, which are given by:

$$D_{43} = \frac{\sum_{i=1}^k n_i D_i^4}{\sum_{i=1}^k n_i D_i^3}$$

where,

$n_i$  = Fog drop quantity of droplets

This average diameter is called the Vol-wtd average diameter. Table 3 shows that the particle size of charged droplets is smaller than that of uncharged droplets. Therefore, particle size improved after the droplets were charged.

Figure 7 shows the distribution of charged droplet size, whereas Fig. 8 shows the distribution of uncharged droplet size. A comparison of the two figures shows that the distribution of charged droplets is more uniform. Therefore, high-pressure electrostatic can improve the distribution of droplet particles.

**Velocity distribution:** Figure 9 shows the distribution of the mean axial velocity of charged and uncharged droplets when the working pressure is 0.3 MPa. Furthermore, the mean axial velocity of charged droplets is faster than that of uncharged droplets, and the velocity distribution is gentler. For the 11 survey points, those that are closer to zero exhibit a greater gap of mean axial velocity between charged and uncharged droplets. Thus, high-pressure electrostatic improves the mean axial velocity of droplets and makes the mean velocity distribution more uniform.

### CONCLUSION

- Charge-to-mass ratio increases with working pressure. Therefore, an appropriate increase in working pressure can improve the charge-to-mass ratio of droplets.

- High-pressure electrostatic can reduce the number and improve the distribution of droplet particles, making them smaller and more evenly distributed. High-pressure electrostatic can also improve and enhance the uniformity of mean velocity distribution.
- The deposition rate of charged droplets is better than that of uncharged droplets because the former adsorb the directional movement on the crops and affect the deposition rate on the underside of leaves.

#### ACKNOWLEDGMENT

This study is financially supported by the National Science Foundation of China (Grant No. 50975125), the Jiangsu province Science Foundation of China (Grant No. BK2011048) and Scientific Research Foundation for senior professionals of Jiangsu University (Grant No.09JDG056). And A Project Funded by the Priority Academic Program Development of Jiangsu Higher Education Institutions (PAPD). The authors also want to express their thanks to those graduate students majored in the Fluid Mechanism and Engineering for their wonderful work.

#### REFERENCES

- Edward, L.S., 2001. Agricultural electrostatic spray application: A review of significant research and development during the 20th century [J]. *J. Elec.*, 51-52(5): 25-42.
- Jia, W.D., B.J. Qiu, A.P. Shi and M. Guohua, 2007. Measurement of agricultural high-voltage electrostatic spraying field by using PDPA [J]. *Trans. Chinese Soc. Agric. Mach.*, 38(12): 66-69.
- Jia, W.D., P.P. Li, B.J. Qiu, X. Fu and X. Xue, 2008. Experimental investigation of droplet diameter and velocity distributions in agricultural electrostatic sprays [J]. *Trans. CSAE*, 24(2): 17-21.
- Kang, C., X.Y. Wang, T.Q. Luo, W. Abdu and Z. Gao, 2007. Experimental study on high-voltage electrostatic spraying locust-killing machine [J]. *Trans. Chinese Soc. Agric. Mach.*, 38(6): 66-70.
- Lv, T.G., 2009. Study of electro-spray system characteristics [J]. *J. Agric. Mechanizat. Res.*, 8: 54-70.
- Shu, Z.R., H.L. Xiong, G.F. Chen *et al.*, 2002. Current situation and development of the research and application of the electrostatic spraying- dusting technique [J]. *J. Shenyang Agric. Univ.*, 33(3): 211-214.
- Wang, Z.T., J.L. Wen, X.Y. Wang *et al.*, 2008. High voltage electrostatic spray [J]. *High Volt. Eng.*, 34(5): 1067-1072.
- Wang, Z.T., J.L. Wen, Y. Chen and Z. Wang, 2004. Theory and application technology improvement of electrostatic atomization research [J]. *Drainage Irrigat. Mach.*, 22(6): 41-44.
- Wen, J.L., J.F. Wang, S.S. Chen and T. Luo, 2003. Experimental research on electrostatic charged spray combustion [J]. *Trans. Chinese Soc. Agric. Mach.*, 34(5): 4-7.
- Yuan, H.Y., Z.S. Ma, H.Q. Qin and X. Zhao, 2000. Experiment and research on high voltage electrode for electrostatic coating on food surface [J]. *Trans. CSAE*, 16(2): 113-115.